

# An ab initio study of the electronic and geometric structures of $\text{Si}_m\text{C}_n^+$ cationic nanoclusters

P. Pradhan and A.K. Ray<sup>a</sup>

Department of Physics, The University of Texas at Arlington, P.O. Box 19059, Arlington, Texas 76019, USA

Received 12 June 2005 / Received in final form 18 September 2005

Published online 20 December 2005 – © EDP Sciences, Società Italiana di Fisica, Springer-Verlag 2005

**Abstract.** The theoretical formalism of local density approximation (LDA) to density functional theory (DFT) has been used to study the electronic and geometric structures of  $\text{Si}_m\text{C}_n^+$  ( $1 \leq m, n \leq 4$ ) cationic clusters. An all electron 6-311++G\*\* basis set has been used and complete geometry optimizations of different possible structures for a specific cluster have been carried out. Binding energies, relative energies, fragmentation energies, vibrational frequencies, and adiabatic ionization potentials of the optimized clusters have been investigated and reported in detail. Results have been compared with other experimental and theoretical results available in the literature.

**PACS.** 31.10.+z Theory of electronic structure, electronic transitions, and chemical binding – 31.15.Ar Ab initio calculations – 31.15.Ew Density-functional theory – 36.40.Qv Stability and fragmentation of clusters

## 1 Introduction

Recent years have seen an explosive interest in computational, experimental, and theoretical studies of atomic and molecular clusters [1–9]. Clusters are distinctly different from their bulk state and exhibit many specific properties, which distinguishes their studies as a completely different branch of science named “Cluster Science”. Large surface to volume ratio and quantum effects resulting from small dimensions are usually prominent in clusters and ideas like ‘super-atoms’, ‘magic numbers’ or ‘fission’ in clusters have prompted a wide class of scientists to study this ‘relatively’ new area of the physical sciences. Growing interests in the stabilities of small clusters and the evolution of bulk properties from cluster properties are also due to the emergence of new areas of research called nanoscience and nanotechnology and the resulting potentials in industrial applications, e.g. for electronic devices, for data storage, or for fostering chemical reactions [10–13]. Among various types of clusters, simple metal and semiconductor clusters continue to be the most important and widely studied clusters, both experimentally and theoretically. In the area of semiconductor clusters, carbon and silicon, though belonging to the same column of the periodic table, vary significantly in their basic chemical and physical properties. A combination of these two materials silicon-carbide (SiC) or carborundum exists in many different poly-types and, in crystalline phase is a very important scientific and technological material. Silicon carbide (SiC)

possesses many favorable properties making it suitable for high-temperature, high-frequency, and high voltage integrated electronics. More specifically, these properties are wide band-gap, high thermal conductivity (better than that for copper at room temperature), high breakdown electric field strength (approximately 10 times that of Si), high saturation drift velocity (higher than GaAs), high thermal stability and chemical inertness.

Our interest in silicon-carbon clusters stems from our recent studies where we have shown that carbon clusters trapped inside medium sized silicon cages gave rise to highly symmetric, stable cage clusters [14]. This work is a continuation of these studies in the area of small cationic silicon-carbon clusters. In the investigation of heteroatomic silicon-carbon clusters, it is probable that some novel bonding arrangements might be observed yielding lowest energy isomers and possibly “magic” SiC clusters. Bulk SiC has a tetragonal bonding of carbon atom with four nearest silicon neighbors. The bond distances for Si–Si and Si–C are 3.08 Å and 1.89 Å respectively. In all probability, this type of bonding will not be observed for SiC clusters. Silicon is known to prefer multidimensional single bonds and carbon can form single, double, and triple bonds.

There has been considerable theoretical studies on the structure and electronic state of neutral  $\text{Si}_m\text{C}_n$  clusters ( $n + m < 9$ ) [15–23], including our recent work [24] in which we have studied small neutral silicon-carbon  $\text{Si}_m\text{C}_n$  ( $1 \leq m, n \leq 4$ ) clusters at the SVWN/6-311++G\*\* level. Various cluster properties such

<sup>a</sup> e-mail: akr@uta.edu

as binding energies, vertical ionization potentials, vertical electron affinities, fragmentation energies, and other electronic structure properties of interest were studied in detail. But time-of-flight mass spectrum experiments usually show the existence of only charged species, thereby increasing the importance of investigating the electronic and structural properties of these ionic species. In this paper we extend our previous work on neutral  $\text{Si}_m\text{C}_n$  clusters to the electronic and geometric structures and associated properties of small cationic silicon-carbon  $\text{Si}_m\text{C}_n^+$  ( $1 \leq m, n \leq 4$ ) clusters.

Most of the previous theoretical studies in the literature for small SiC clusters employ small basis sets with no diffuse functions. The lack of diffuse functions can affect the quality of the calculations, particularly the energetics. In fact, there is a continuing debate regarding the correct ground state structures for these clusters with close lying cyclic and linear isomers. *Ours is the first attempt to study these clusters on an equal footing from a completely ab initio point of view with a large basis set with added diffuse functions. We also present detailed results on cohesive energies and fragmentation energies and report for the first time results on adiabatic ionization potentials for small  $\text{Si}_m\text{C}_n$  clusters. Of course, wherever possible, we compare our results with results available in the literature.* First principles simulations, based on local density approximation to density functional theory (LDA-DFT), have proved to be a reliable and computationally tractable tool in quantum chemistry and condensed matter physics [25–27]. This formalism is used here to investigate mixed silicon-carbon clusters  $\text{Si}_m\text{C}_n^+$  ( $1 \leq m, n \leq 4$ ).

## 2 Computational details

One of the primary considerations involved in these calculations is the determination of the methodology, specifically the form of the exchange-correlation potential and the type of basis set to be used. Our previous work on SiC neutral clusters have indicated that the choice of the SVWN functional [28] with an all-electron 6-311++G\*\* basis set [29] yields very reasonable results [24]. This, combined with the fact that comparisons with the electronic and geometric structure properties of equivalent neutral clusters are helpful and necessary, have prompted us to use these basis set and functional for all  $\text{Si}_m\text{C}_n^+$  cationic clusters as well. The binding energy per atom for the cationic clusters is calculated from

$$E_b = \frac{[E(\text{Si}^+) + (m-1)E(\text{Si}) + nE(\text{C})] - [E(\text{Si}_m\text{C}_n^+)]}{m+n} \quad (1a)$$

$$E_b = \frac{[mE(\text{Si}) + (n-1)E(\text{C}) + E(\text{C}^+)] - [E(\text{Si}_m\text{C}_n^+)]}{m+n} \quad (1b)$$

where  $E(\text{Si}_m\text{C}_n^+)$  is the optimized total energy of the cluster. In these, we have assumed that the extra charge can go either to the Si atom or to the C atom. The lower of the

two energies is taken to be the binding energy of the cluster and we have found, as detailed below, that the extra charge usually goes to the Si atom.

The fragmentation energy of the clusters into different binary channels is calculated from

$$E_{n \rightarrow (n-m)+m}^+ = E_{n-m}^+ + E_m - E_n^+, \quad (1 \leq n, m \leq 4) \quad (2)$$

and the adiabatic ionization potential is calculated from

$$AIP = E(\text{Si}_m\text{C}_n^+) - E(\text{Si}_m\text{C}_n) \quad (3)$$

where  $E(\text{Si}_m\text{C}_n^+)$  is the total energy of the cationic and the corresponding neutral cluster at their respective optimized geometries. All computations have been performed using the *Gaussian03* suite of programs [30] at the University of Texas at Arlington supercomputing facilities.

## 3 Results

Since usually experimental data correspond to the most stable isomers, our discussion will focus on the structures and properties of the most stable clusters and isomers nearly iso-energetic with these and some other selected isomers of special interest. However, other isomers will also be discussed briefly. For the sake of brevity, we have represented here in Figures 1–16 and Tables 1–16 the results from only the three most stable isomers for each cluster, with the bond lengths in Angstroms. However, all the isomers are included in the discussion. The structures are denoted by *C.m.n.i*, where *i* runs from 1 to the number of isomers of a particular cluster in decreasing order of stability. Thus, for example, the most stable  $\text{Si}_4\text{C}_4^+$  cationic cluster is indicated in Figure 16 by C.4.4.1. All structures are Bery geometry and spin-optimized [31]. Tables 1–16 give the electronic state, binding energy per atom, relative energy, and adiabatic ionization potential (all in eV) for each structure for the three most stable isomers. Table 17 compares our theoretical vibrational frequencies in  $\text{cm}^{-1}$  with the results reported in the literature where available. In the following sections, we discuss the results in detail.

Before explaining the geometries of  $\text{Si}_m\text{C}_n^+$  ( $1 \leq m, n \leq 4$ ) clusters, we present very briefly our results on the ground state of *neutral*  $\text{Si}_m\text{C}_n$  ( $1 \leq m, n \leq 4$ ) clusters. A detailed description is provided in reference [24]. Three atoms species  $\text{SiC}_2$  and  $\text{Si}_2\text{C}$  have a  $\text{C}_{2v}$  symmetry triangle-shaped structure as the ground state. In case of four atoms species, the ground state for  $\text{SiC}_3$  cluster is a Si-terminated linear structure,  $\text{Si}_2\text{C}_2$  cluster has a cyclic rhombus with  $^1\text{A}_g$  state and  $\text{Si}_3\text{C}$  cluster is a  $\text{C}_{2v}$  symmetry rhomboidal structure with a  $\text{Si}_2\text{C}$  sub-molecule. In the five atom species, the ground states for  $\text{SiC}_4$  and  $\text{Si}_2\text{C}_3$  clusters are Si-terminated chains. Among the silicon-rich clusters,  $\text{Si}_3\text{C}_2$  is a planar pentagon with a  $\text{C}_2$  sub-molecule and  $\text{Si}_4\text{C}$  has a distorted trigonal bipyramid as the ground state structure. Among the six atom species, except for  $\text{Si}_2\text{C}_4$  cluster, where the ground state is a linear chain with terminal silicon atoms, both  $\text{Si}_3\text{C}_3$  and  $\text{Si}_4\text{C}_2$  clusters show 3D structures as ground states.

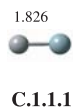
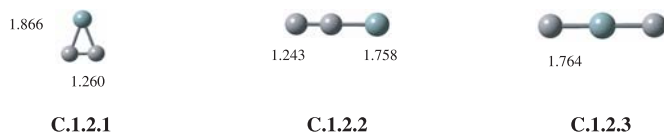


Fig. 1. SiC cationic cluster.

Fig. 2.  $\text{SiC}_2$  cationic clusters.

Seven atom clusters  $\text{Si}_3\text{C}_4$  and  $\text{Si}_3\text{C}_4$  have distorted planar structures as ground states and eight atom cluster  $\text{Si}_4\text{C}_4$  has 3D pyramid-like structure in  $^1\text{A}_1$  electronic state as the most stable structure. In general, we found a strong tendency for the carbon-rich species to be chainlike whereas the silicon-rich species are either planar or 3D. Moreover, the ratio of  $sp^2$  to  $sp^3$  hybridization, formation of CC bonds and several SiC bonds and coordination of atoms directly affected the geometry of a specific cluster.

### 3.1 $\text{SiC}_n$ cations

#### 3.1.1 $\text{SiC}^+$

The  $\text{SiC}^+$  dimer (Fig. C.1.1.1) has  $^4\Sigma$  electronic state. The bond length is 1.826 Å. Mulliken charge distribution analysis [32] shows that the silicon atom carries most of the positive charge ( $0.853e$ ) and carbon atom a negligible charge ( $0.146e$ ). The dipole moment is 1.254 D. It is apparent that due to the detachment of an electron from a bonding or an anti-bonding orbital we see an increase in the Si–C bond length and a decrease in the vibrational frequency as compared to the corresponding quantities for the neutral cluster.

#### 3.1.2 $\text{SiC}_2^+$

Flores et al. [33] conducted ab initio studies at both HF and correlated levels of theory of this cluster with a 6-31G\* basis set. At the HF and at the configuration-interaction-size-consistent CISD (SCC) levels, the linear structure was found to be most stable but at the fourth-order many body perturbation theory (MP4) level, the cyclic structure with  $\text{C}_{2v}$  symmetry was the ground state. Lavendy et al. [34] studied  $\text{SiC}_2^+$  at different levels of theory with 6-311G\* and aug-cc-pVTZ basis sets. With the first basis set, the linear set was found to be the ground state at the B3LYP and CCSD(T) levels of theory whereas with the second basis set, the results are mixed at the

**Table 1.** Electronic state, relative energy, binding energy/atom, adiabatic ionization potential (all in eV) for  $\text{SiC}^+$  cluster.

Structure	State	$\Delta E$	$E_b$	$AIP$
C.1.1.1	$^4\Sigma$	0.00	2.279	9.612
				8.7(0.2) [38]

**Table 2.** Electronic states, relative energies, binding energies/atom, and adiabatic ionization potentials (all in eV) for  $\text{SiC}_2^+$  clusters.

Structure	State	$\Delta E$	$E_b$	$AIP$
C.1.2.1	$^2\text{A}_1$	0.000	4.568	10.387
C.1.2.2	$^2\Sigma$	0.116	4.530	10.321
C.1.2.3	$^2\Sigma_u$	6.553	2.384	10.783

SVWN, B3LYP, B3PW91, CCSD (T) and MRCI levels. Wu et al. [35] with a smaller 6-31G\* basis set and B3LYP level of theory obtained linear state as the ground state. All these studies clearly indicate the importance of electron correlation and consistency in the level of theory for such systems in order to obtain the true ground states of  $\text{Si}_m\text{C}_n^+$  clusters. Experimental studies by Michalopoulos et al. [36] and Parent [37] on  $\text{SiC}_2^+$  also remain inconclusive about the geometric structure of this cluster. We studied all three possible isomers and conclude that the ground state of  $\text{SiC}_2^+$  (Fig. C.1.2.1) is cyclic with an apical angle of  $39.4^\circ$  in the  $^2\text{A}_1$  electronic state. The Si–C bond length is 1.866 Å (greater than that of the corresponding neutral structure 1.837 Å) and C–C bond length is 1.260 Å (suggesting a probable double bond). Mulliken charge distribution analysis indicates that the silicon atom carries most of the positive charge ( $0.763e$ ) and carbon atoms, a small charge ( $0.118e$ ). The Si-terminated linear geometry (Fig. C.1.2.2) is just 0.116 eV above the ground state followed by a centro-symmetric linear structure (Fig. C.1.2.3) 6.553 eV above the ground state. The same trend was observed in the case of neutral clusters. Frequency analysis (Tab. 17) indicates that our vibrational frequencies are in good agreement with the results of Lavendy et al. We do observe though that both cyclic and linear isomers have all real frequencies.

#### 3.1.3 $\text{SiC}_3^+$

An ab initio study by Lavendy et al. [34] at various levels of theory using 6-311G\* and aug-cc-pVTZ basis sets found a rhomboidal  $\text{C}_{2v}$  ( $^2\text{A}_1$ ) structure as the ground state. We also conclude that a rhomboidal structure (Fig. C.1.3.1) in  $^2\text{A}_1$  electronic state is the ground state. The  $\text{C}_3$  submolecule has bond lengths of 1.351 Å each, Si–C bond lengths are 1.930 Å (longer than the typical single bond value) and trans-annular bond angle of  $67.5^\circ$ . We note that for the neutral  $\text{SiC}_3$  cluster (where a Si-terminated chain is the ground minimum) this structure was the third most stable isomer and ionization led to the stabilization of

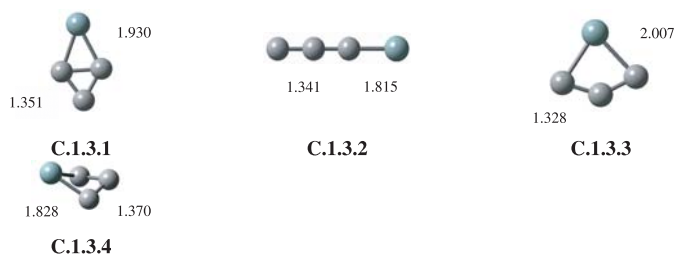


Fig. 3. SiC<sub>3</sub> cationic clusters.

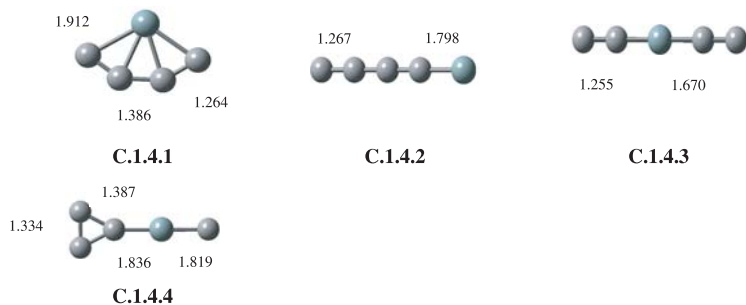


Fig. 4. SiC<sub>4</sub> cationic clusters.

this structure into the cationic ground minimum. Mulliken charge distribution shows strong electrostatic interaction between Si and C<sub>3</sub> sub-molecule, as most of the positive charge is carried by the apical silicon atom (0.71*e*). Next, lying 0.637 eV above is a silicon-terminated chain (Fig. C.1.3.2) with C–C bond lengths of 1.341 Å each and SiC bond length of 1.815 Å. The energy difference in the neutral linear and cyclic isomers (0.642 eV) is more than the cationic isomers and the structure ordering is reversed. The dipole moment is 4 D for the cationic linear isomer as compared to 0.956 D for the cyclic minimum. For the linear structure, the charge on the silicon atom (0.636*e*) and on the neighboring carbon atom (−3.326*e*) renders a strong ionic character to the Si–C bond. Following the energetics, close lying 0.727 eV above the minimum is another rhomboidal structure (Fig. C.1.3.3), with a trans-annular bond angle of 135.2°. A 3D rhomboidal structure (Fig. C.3.1.4) lies 2.731 eV above the ground state. Frequency analysis (Tab. 17) indicates that our vibrational frequencies are in good agreement with the results of Lavendy et al. [34].

### 3.1.4 SiC<sub>4</sub><sup>+</sup>

B3LYP/6-31G\* study by Pascoli and Lavendy [34] found a Si-terminated linear structure in <sup>2</sup>Σ<sup>+</sup> electronic state (C<sub>∞v</sub> symmetry) to be the global minimum with Si-capped bent C<sub>4</sub> chain structure lying 2 kcal/mol above the ground state. We explored these as well as various other structures and conclude instead that the fan-shaped planar structure (Fig. C.1.4.1), derived essentially from SiC<sub>3</sub><sup>+</sup> isomer (Fig. C.1.3.3) to be the ground state structure. The binding energy per atom increases from 5.338 eV (SiC<sub>3</sub><sup>+</sup>) to 5.617 eV (SiC<sub>4</sub><sup>+</sup>) by the addition of an extra carbon atom. This structure has Si–C bonds

Table 3. Electronic states, relative energies, binding energies/atom, and adiabatic ionization potentials (all in eV) for SiC<sub>3</sub><sup>+</sup> clusters.

Structure	State	$\Delta E$	$E_b$	$AIP$
C.1.3.1	<sup>2</sup> A <sub>1</sub>	0.000	5.338	8.554
C.1.3.2	<sup>2</sup> Π	0.637	5.179	9.833
C.1.3.3	<sup>2</sup> B <sub>2</sub>	0.727	5.157	9.635
C.1.3.4	<sup>4</sup> A	2.731	4.656	10.862

Table 4. Electronic states, relative energies, binding energies/atom, and adiabatic ionization potentials (all in eV) for SiC<sub>4</sub><sup>+</sup> clusters.

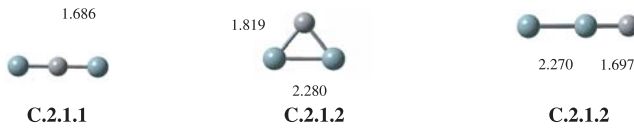
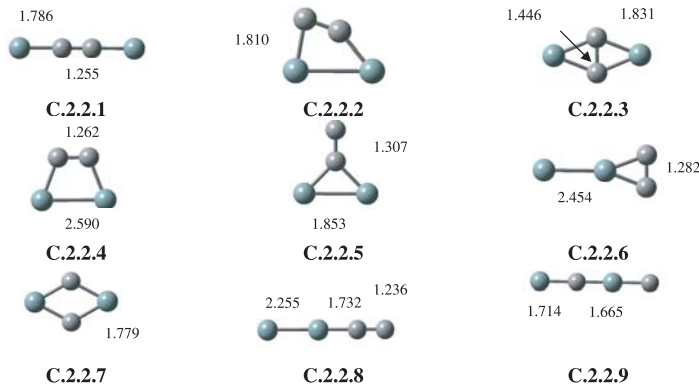
Structure	State	$\Delta E$	$E_b$	$AIP$
C.1.4.1	<sup>2</sup> A <sub>1</sub>	0.000	5.617	10.445
C.1.4.2	<sup>2</sup> Σ	1.051	5.407	12.377
C.1.4.4	<sup>2</sup> Σ <sub>u</sub>	2.312	5.155	10.635
C.1.4.4	<sup>2</sup> B <sub>1</sub>	4.716	4.674	9.986

of 1.912 Å and 1.970 Å (slightly higher than the typical Si–C single bond value) and C–C bond lengths between 1.264–1.386 Å. Several strong Si–C bonds contribute towards the stability of this particular geometry. Mulliken charge distribution shows that the silicon atom bears most of the charge (0.756*e*) and terminal carbon atoms carries slight charge of (0.116*e*) each. The Si-terminated linear chain (Fig. C.1.4.2) is 1.051 eV above the minimum, with Si–C linkage of 1.798 Å and C–C bond lengths are 1.267 Å, 1.291 Å, and 1.282 Å. There are few other low lying states but mostly planar or linear showing the preference of these C-rich clusters not to take part in multiple bonding. All these structures have doublet states. Frequency analysis (Tab. 17) gives our vibrational frequencies, all real, for the predicted fan-shaped ground minimum. The existence of all real frequencies tends to indicate that ours indeed is the global minimum structure. Pascoli and Lavendy [34] obtained negative frequencies for this structure.

## 3.2 Si<sub>2</sub>C<sub>n</sub> cations

### 3.2.1 Si<sub>2</sub>C<sup>+</sup>

MP2 optimizations by Boldyrev et al. [38] indicated two linear geometries in <sup>2</sup>Π<sub>u</sub> and <sup>2</sup>Σ<sub>u</sub> states, with an energy difference of the order of 4.6 ± 4 kcal/mol. Lavendy et al. [34] showed with an AVTZ basis set that, the <sup>2</sup>Σ<sub>u</sub> (Linear) – <sup>2</sup>B<sub>2</sub> (cyclic) transition energy is quite small at SVWN and B3LYP levels, 1.1 kcal/mol (B3PW91), 1 kcal/mol (CCSD(T)), and 0.5 kcal/mol (MRCI) in favor of the cyclic isomer. With a 6-311G\* basis set, the linear structure was the ground state and the authors concluded that the basis set was not flexible or polarized enough. Jiang et al. [35], using B3LYP/6-311G (d) method, obtained the <sup>2</sup>Σ<sub>u</sub><sup>+</sup> state linear isomer to be 187.72 kJ/mol

Fig. 5.  $\text{Si}_2\text{C}$  cationic clusters.Fig. 6.  $\text{Si}_2\text{C}_2$  cationic clusters.

more stable than the  $^4\text{B}_2$  state cyclic isomer. Our results indicate that the linear isomer is 2.054 eV below the cyclic isomer. Grev and Schaefer [16] mentioned in the case of neutral  $\text{Si}_2\text{C}$  clusters that addition of polarization functions can lead to a bent structure even at HF level. Our basis set has added diffuse and polarization functions and we believe that the predicted ground state for  $\text{Si}_2\text{C}^+$  cation is correct. Another carbon terminated asymmetric linear structure (Fig. C.2.1.2) is about 3.821 eV above the global minimum. Frequency analysis (Tab. 17) gives real vibrational frequencies for the predicted linear ground minimum. Our theoretical frequencies do not agree well with the results by Lavendy et al. [34], possibly due to the differences in the basis set and ground state geometries and experimental results will be very welcome.

### 3.2.2 $\text{Si}_2\text{C}_2^+$

Ignatyev and Schaefer [16] at ROHF, CISD, and UB3LYP levels with DZP basis set identified three low lying minima. The ground state was a linear chain followed by a distorted rhomboid structure lying 17 kcal/mol above the minimum. Lavendy et al. [34] at various levels of theory like B3LYP, B3PW91, and SVWN using 6-311G\* basis set found the lowest lying structure to be a linear chain with carbon atoms between silicon atoms and a cyclic  $^2\text{A}_1$  rhombus structure was found to be the second most stable structure, the difference in energies being 20 kcal/mol. Mass spectroscopy experiments [37] reveal unusual kinetic behavior (i.e. non-linearity of the

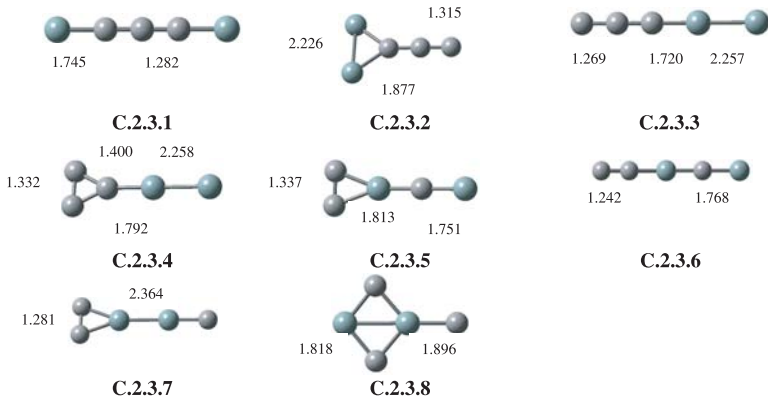
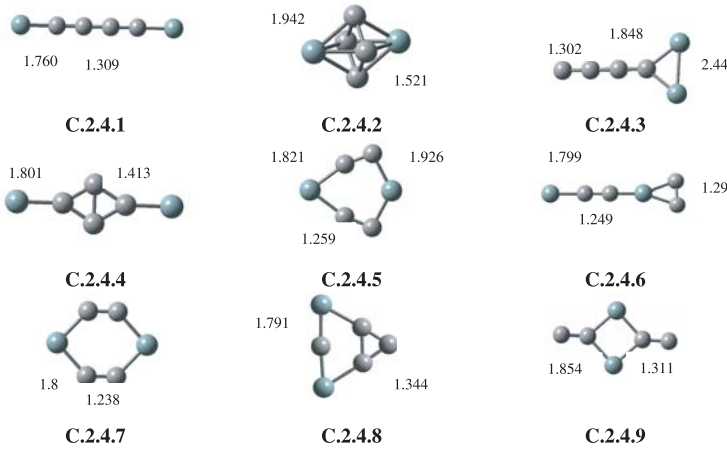
**Table 5.** Electronic states, relative energies, binding energies/atom, and adiabatic ionization potentials (all in eV) for  $\text{Si}_2\text{C}^+$  clusters.

Structure	State	$\Delta E$	$E_b$	$AIP$
C.2.1.1	$^2\Sigma_u$	0.00	4.029	9.626
				9.2(0.2) [38]
C.2.1.2	$^4\text{B}_2$	2.054	3.344	11.681
C.2.1.3	$^2\Sigma$	3.821	2.755	10.083

**Table 6.** Electronic states, relative energies, binding energies/atom, and adiabatic ionization potentials (all in eV) for  $\text{Si}_2\text{C}_2^+$  clusters.

Structure	State	$\Delta E$	$E_b$	$AIP$
C.2.2.1	$^2\Pi_g$	0.00	5.125	8.259
				8.24(0.20) [37]
C.2.2.2	$^2\text{A}'$	0.498	5.001	8.691
C.2.2.3	$^2\text{A}_1$	1.015	4.872	9.547
				9.25(0.20) [37]
C.2.2.4	$^2\text{A}_1$	1.104	4.849	7.794
C.2.2.5	$^2\text{A}_1$	1.714	4.697	8.744
C.2.2.6	$^2\text{B}_2$	3.142	4.340	9.202
C.2.2.7	$^2\text{B}_{1g}$	3.294	4.302	8.872
C.2.2.8	$^4\Sigma$	3.818	4.171	9.675
C.2.2.9	$^4\Sigma$	5.194	3.827	9.552

first order plot) exhibited by  $\text{Si}_2\text{C}_2^+$  cation. A possible reason for this behavior maybe the co-existence of two forms of this cation. We studied various geometries for this cation, essentially based on the neutral  $\text{Si}_2\text{C}_2$  cluster [24]. The low-lying stable six isomers are given in Figure 6. The most stable neutral  $\text{Si}_2\text{C}_2$  isomer was a planar rhombus (1.422 Å, 1.834 Å) and the ionization of this isomer led to a  $^2\text{A}_g$  structure (Fig. C.2.2.3) with an increase in C–C distance to 1.446 Å and a decrease in Si–C distance to 1.831 Å. This structure lies about 1.015 eV above the ground state linear isomer. Detachment of an electron from the neutral  $\text{Si}_2\text{C}_2$  linear isomer (1.276 Å, 1.737 Å) led to the most stable cationic ground state, a centrosymmetric linear chain (Fig. C.2.2.1) with  $^2\Pi_g$  electronic state. Ionization led to the shortening of the C–C bond length to 1.255 Å, between the typical double bond (1.35 Å in ethylene) and triple bond (1.21 Å in acetylene). The Si–C bond length increased to 1.786 Å indicating a single bond. Thus, ionization of this cluster in fact reduces the electrostatic repulsion and led to the preference for  $sp$  hybridization. Mulliken charge distribution shows that the two silicon atoms bear equal charges of about 0.474e each and the carbon atoms carry slight positive charge of about 0.025e each. Thus, the nearest-neighbor electrostatic repulsion is not very significant. On the other hand, Lavendy et al. [34] found that silicon atoms carried charges of 0.8e each and the carbon atoms  $-0.3e$  each. A planar distorted trapezoidal structure (Fig. C.2.2.2) is the second most stable structure and is just 0.498 eV above the ground state. The C–C bond length is 1.286 Å

Fig. 7.  $\text{Si}_2\text{C}_3$  cationic clusters.Fig. 8.  $\text{Si}_2\text{C}_4$  cationic clusters.

(0.03 Å shorter than the corresponding neutral geometry). Among the other low-lying isomers are a trapezoid (Fig. C.2.2.4) and two T-shaped structures (Figs. C.2.2.5, C.2.2.6) as shown in Figure 6. The energetic ordering is well in agreement with the B3LYP/6-311G (d) results by Jiang et al. [35]. We note that, in general, the  $\text{Si}_2\text{C}_2$  cluster, with equal numbers of silicon and carbon atoms, favors planar geometry. Frequency analysis confirms that the linear isomer with all real vibrational frequencies is in fact the ground state. Our calculated frequencies (Tab. 17) are in fair agreement with other results in the literature.

### 3.2.3 $\text{Si}_2\text{C}_3^+$

A B3LYP/6-311G\* study by Pascoli and Lavendy [34] for this cluster reports only two isomers, one symmetric linear arrangement with ( $D_{\infty h}$ ,  $^2\Pi_g$ ) as the lowest energy isomer followed by a T-shaped structure ( $C_{2v}$ ,  $^4B_2$ ) about 81 kcal/mol above the minimum. We also conclude that, the most stable isomer (Fig. C.2.3.1) is the Si-terminated linear chain in  $^2\Pi_g$  electronic state. The Si–C linkage is 1.745 Å and the C–C bonds are 1.282 Å suggesting a probable double bond. Mulliken charge distribution analysis shows that the two terminal silicon atoms carry slightly positive charges of (0.414e) each. Among

**Table 7.** Electronic states, relative energies, binding energies/atom, and adiabatic ionization potentials (all in eV) for  $\text{Si}_2\text{C}_3^+$  clusters.

Structure	State	$\Delta E$	$E_b$	AIP
C.2.3.1	$^2\Pi_g$	0.000	5.673	9.034
C.2.3.2	$^2A_1$	2.891	5.095	9.261
C.2.3.3	$^2\Pi_g$	3.865	4.900	9.386
C.2.3.4	$^2B_1$	4.476	4.778	9.033
C.2.3.5	$^4A_1$	5.682	4.536	12.202
C.2.3.6	$^2\Pi_g$	6.237	4.425	12.334
C.2.3.7	$^2B_1$	7.480	4.177	9.888
C.2.3.8	$^2A_1$	9.570	3.759	9.407

**Table 8.** Electronic states, relative energies, binding energies/atom, and adiabatic ionization potentials (all in eV) for  $\text{Si}_2\text{C}_4^+$  clusters.

Structure	State	$\Delta E$	$E_b$	AIP
C.2.4.1	$^2\Sigma_u$	0.000	6.089	7.962
C.2.4.2	$^2A_g$	2.071	5.744	8.068
C.2.4.3	$^2A_1$	2.198	5.722	8.671
C.2.4.4	$^2B_{2u}$	2.554	5.663	7.463
C.2.4.5	$^2A_1$	2.557	5.663	8.750
C.2.4.6	$^2B_2$	3.410	5.520	8.430
C.2.4.7	$^4B_{3u}$	3.501	5.505	9.364
C.2.4.8	$^2A_1$	3.839	5.449	9.097
C.2.4.9	$^2B_{2u}$	4.025	5.418	9.811

the carbon atoms, the centermost carbon atom bears a large charge of (2.574e) whereas the other two carbon atoms carry fairly large negative charge of (−1.201e) each. Similar trend was observed in case of neutral  $\text{Si}_2\text{C}_3$  cluster. We can see a strong oscillation of charge along the chain. Next, we observed several low-lying isomers (Fig. 7) for this cluster. Most favored geometries were linear or planar T-shaped Si-terminated structures. This indicates silicon non-preference to participate in multiple bonding (*sp* hybridization). In Table 17, we have compared our vibrational frequencies with other published in the literature [34]. For the ground state structure, we detected some additional lower modes of vibrational frequencies, but in general the predicted values compare favorably. For all other isomers, we found one or two imaginary frequencies indicating they are possibly saddle points on the potential energy curve.

### 3.2.4 $\text{Si}_2\text{C}_4^+$

The ground state structure for the  $\text{Si}_2\text{C}_4^+$  cation is a linear chain with terminal silicon atoms and a  $C_4$  chain in between (Fig. C.2.4.1). It is derived by the detachment of an electron from the ground state  $\text{Si}_2\text{C}_4$  cluster also of the same geometry. Ionization led to a change

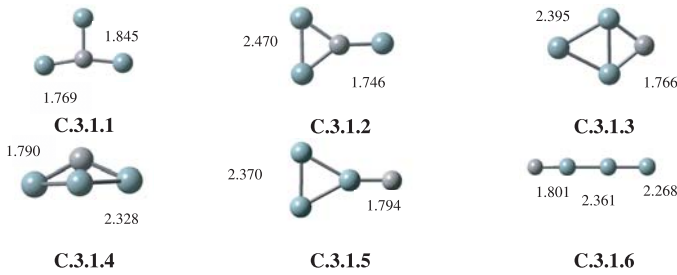


Fig. 9.  $\text{Si}_3\text{C}$  cationic clusters.

in the C–C bond lengths, the lengths being 1.255 Å, 1.309 Å, and 1.255 Å for the cation, as opposed to 1.274 Å, 1.291 Å, and 1.274 Å for the neutral cluster. Mulliken charge distribution analysis shows that the two terminal silicon atoms bear slightly positive charges of  $(0.383e)$  each. Among the carbon atoms, the center-most two carbon atoms bear a large charge of  $(1.705e)$  each whereas the other two carbon atoms carry large negative charge of  $(-1.588e)$  each. We find strong ionic bonding in the terminal Si–C atoms. B3LYP/6-311G\* study by Pascoli and Lavendy [34] predicts the same ground state, but the next stable isomer is a Si-capped bi-cyclic  $\text{C}_4$  structure located 72 kcal/mol above the ground minimum. Our studies predict two more intermediate states before the Si-capped bi-cyclic  $\text{C}_4$  structure 2.554 eV above the minimum (Fig. C.2.4.4). Lying just 2.071 eV above the ground state is a 3D structure (Fig. C.2.4.2) followed by a T-shape structure (Fig. C.2.4.3) with three C–C bonds (1.302 Å, 1.271 Å, 1.309 Å), and 2.198 eV above than the stable minima. A distorted hexagonal ring (Fig. C.2.4.5), derived essentially from  $\text{C}_6$  ground state is 2.557 eV above the ground minima. Some of the other low-lying isomers are also given in Figure 8. Frequency analysis (Tab. 17) indicates that our vibrational frequencies are in good agreement with theoretical results published in the literature.

### 3.3 $\text{Si}_3\text{C}_n$ cations

#### 3.3.1 $\text{Si}_3\text{C}^+$

B3LYP/6-311G\* study by Jiang et al. [35] predicts the ground state structure to be a rhomboidal  $\text{C}_{2v}$  structure with two equivalent silicon atoms and a trans-annular Si–C bond, similar to the neutral  $\text{Si}_3\text{C}$  cluster. On the other hand, Lavendy et al. [34] at B3LYP, B3PW91, SVWN // 6-311G\* level and Boldyrev et al. [38] at MP2 (full)/6-311+G\* level obtained a T-shaped structure with central carbon atom to be most stable. We studied various geometries and find that in fact a T-shaped structure with central carbon atom surrounded by three silicon atoms (Fig. C.3.1.1) is the ground state. This can be explained as a result of ionization of the neutral rhomboidal isomer which led to a stretching of the Si–C linkages (1.769 Å, 1.769 Å, 1.845 Å). Strong interaction between the terminal and bridged silicon atoms thus further leads

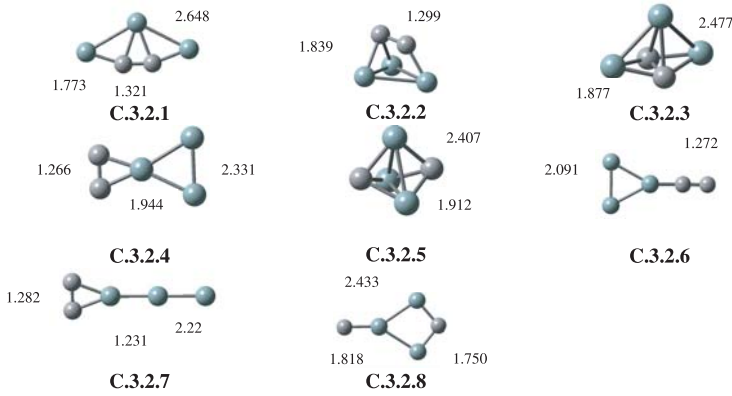
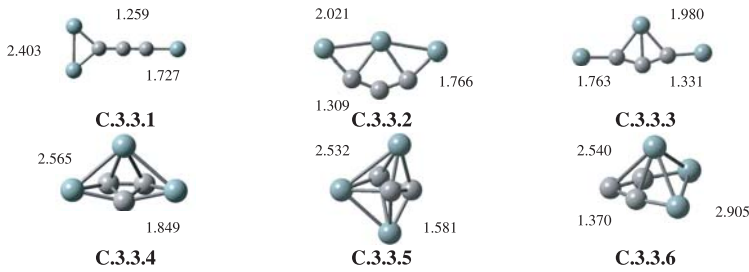
Table 9. Electronic states, relative energies, binding energies/atom, and adiabatic ionization potentials (all in eV) for  $\text{Si}_3\text{C}^+$  clusters.

Structure	State	$\Delta E$	$E_b$	$AIP$
C.3.1.1	$^2\text{B}_2$	0.000	4.462	8.679
				7.8(0.2) [38]
C.3.1.2	$^2\text{A}_1$	0.027	4.455	7.645
C.3.1.3	$^2\text{A}_1$	1.621	4.056	8.212
C.3.1.4	$^4\text{A}$	2.771	3.769	9.317
C.3.1.5	$^2\text{A}_1$	5.032	3.204	8.962
C.3.1.6	$^2\Pi_g$	6.151	2.964	8.989

to the breaking of stretched Si–Si bonds and separation into a separate  $\text{Si}_2\text{C}$  sub-molecule with a Si–C–Si angle of  $164.4^\circ$ . Mulliken charge distribution analysis indicates the two silicon atoms in the  $\text{Si}_2\text{C}$  sub-molecule bear charge of  $(0.48e)$  each. The remaining silicon and carbon atoms carry almost equal and opposite charges of  $(0.339e)$  and  $(-0.301e)$  respectively. Next, 0.027 eV above the minimum is a close-lying T-shaped structure with a  $\text{Si}_2\text{C}$  sub-molecule and silicon on top (Fig. C.3.1.2). The  $\text{Si}_2\text{C}$  sub-molecule has a Si–C–Si angle of  $85.07^\circ$ . A rhomboidal  $\text{C}_{2v}$  isomer (Fig. C.3.1.3) with a  $\text{Si}_3$  silicon sub-molecule is 1.621 eV above the minimum. A few other isomers are given in Figure 9. As observed in case of the neutral  $\text{Si}_3\text{C}$  cluster, carbon-terminated chain cluster (Fig. C.3.1.6) is the least stable structure among all the clusters considered in this group. In general, we conclude that a cluster with more Si–C linkage or a cluster with  $\text{Si}_2\text{C}$  sub-molecule is more energetically preferred than the one with  $\text{Si}_3$  sub-molecule. Also, silicon-terminated chains are energetically preferred over carbon-terminated clusters. The bonding preference thus appears to be in the order Si–C and Si–Si. Frequency analysis (Tab. 17) indicates that our vibrational frequencies are in good agreement with other theoretical results.

#### 3.3.2 $\text{Si}_3\text{C}_2^+$

We spin-optimized various geometries based on the neutral isomers for this cation. We conclude, in agreement with Pascoli and Lavendy [34] and Jiang et al. [35], that a planar pentagon with a  $\text{C}_2$  sub molecule (Fig. C.3.2.1) is the ground state structure showing strong multi-center bonding. The same structure was found to be the ground state in case of the neutral  $\text{Si}_3\text{C}_2$  cluster. The two Si–C bonds of 1.773 Å (typical double bond) and another two Si–C bonds of 1.959 Å (typical single bond) each increased upon ionization (1.727 Å and 1.909 Å for neutral  $\text{Si}_3\text{C}_2$  cluster). The C–C bond shortened to 1.321 Å. Several Si–C bonds along with a stronger C–C bond contribute towards the stability of this cluster. The Si–Si bonds of 2.648 Å are stretched and are almost too weak for any bonding. Mulliken charge distribution shows the three silicon atoms share all of the charge ( $0.357e$ ,  $0.319e$ ,  $0.319e$ ) whereas in case of the neutral cluster, carbons atoms gained some negative charge.

Fig. 10.  $\text{Si}_3\text{C}_2$  cationic clusters.Fig. 11.  $\text{Si}_3\text{C}_3$  cationic clusters.

At this point, our results differ in energetic ordering from the previous two studies [34,35]. We find several intermediate isomers between the ground minimum and the Si-capped bi-cyclic ring observed by others as next most stable structure. The next stable structure (Fig. C.3.2.2) is a distorted 3D trapezoid. The two next stable structures are a prism (Fig. C.3.2.3) lying 2.733 eV and a planar dumbbell-shaped structure (Fig. C.3.2.4) lying 3.848 eV above the global minimum. Other less favored structures are also shown in Figure 10. We note again that the stability of a cluster depends on the formation of strong C–C and Si–C bonds, which are more energetically favorable than the Si–Si bonds. Frequency analysis (Tab. 17) indicates that our vibrational frequencies are in fair agreement with other theoretical results.

### 3.3.3 $\text{Si}_3\text{C}_3^+$

Lavendy et al. [34] reported the global minimum energy isomer as a distorted  $\text{SiC}_3\text{Si}$  chain capped by a Si atom. We obtained this isomer (Fig. C.3.3.3) to be 0.386 eV above the ground state planar T-shaped structure (Fig. C.3.3.1). Next, 0.37 eV above is a planar fan-shaped structure (Fig. C.3.3.2). All these three structures have real vibrational frequencies. This indicates that the two close lying isomers are local minima. As compared to the ground state structure with a dipole moment

**Table 10.** Electronic states, relative energies, binding energies/atom, and adiabatic ionization potentials (all in eV) for  $\text{Si}_3\text{C}_2^+$  clusters.

Structure	State	$\Delta E$	$E_b$	$AIP$
C.3.2.1	$^2A_1$	0.00	5.185	8.144
C.3.2.2	$^4A$	2.438	4.699	9.216
C.3.2.3	$^2B_1$	2.733	4.639	8.491
C.3.2.4	$^2A_1$	3.848	4.416	8.887
C.3.2.5	$^4A_2$	4.042	4.377	9.340
C.3.2.6	$^2A_1$	4.087	4.368	9.153
C.3.2.7	$^2B_1$	4.694	4.246	9.058
C.3.2.8	$^4A_2$	6.193	3.947	8.844

**Table 11.** Electronic states, relative energies, binding energies/atom, and adiabatic ionization potentials (all in eV) for  $\text{Si}_3\text{C}_3^+$  clusters.

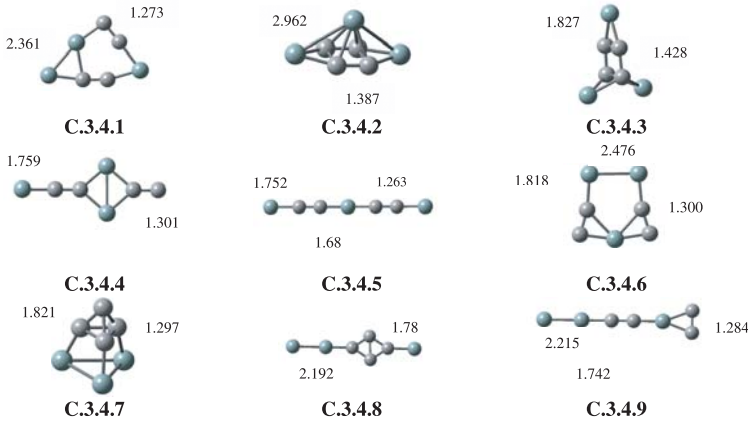
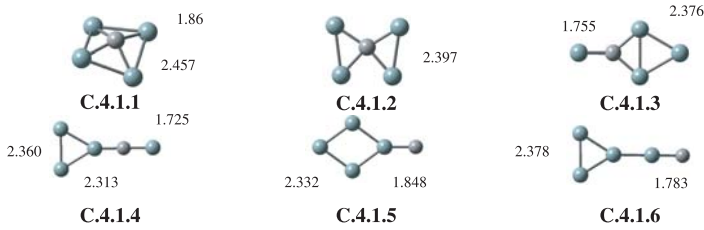
Structure	State	$\Delta E$	$E_b$	$AIP$
C.3.3.1	$^2A_1$	0.000	5.576	7.673
C.3.3.2	$^2B_1$	0.370	5.515	7.891
C.3.3.3	$^2A_1$	0.386	5.512	7.117
C.3.3.4	$^2A$	1.194	5.377	9.297
C.3.3.5	$^2A$	1.534	5.321	7.522
C.3.3.6	$^2A$	1.845	5.269	9.151
C.3.3.7	$^4A$	2.557	5.150	8.907

of 0.937 D, both of these structures have higher dipole moments of 1.149 D (Fig. C.3.3.2) and 1.182 D (Fig. C.3.3.3). A distorted pentagonal pyramid with a  $\text{C}_3$  sub-molecule (Fig. C.3.3.4) observed as the ground state in case of neutral  $\text{Si}_3\text{C}_3$  cluster is 1.194 eV above the cationic minimum. Here C–C and Si–Si bonds appear to be stretched as compared to the neutral cluster. The Si–C bonds of 1.849 Å lie within the range for Si–C single bond length. Thus,  $\text{Si}_3\text{C}_3^+$  cation in contrast to its neutral counterpart prefers planar geometries. The frequencies are shown in Table 17.

### 3.3.4 $\text{Si}_3\text{C}_4^+$

As far as we know, *no* results have been reported on these clusters, theoretically or experimentally. We examined various planar, quasi-planar and 3D structures based on the geometries of the neutral clusters [24]. We conclude that a slightly distorted pyramid-shaped planar cyclic structure (Fig. C.3.4.1) is the ground state structure. The same structure was observed as the ground state structure in the case of neutral  $\text{Si}_3\text{C}_4$  clusters. The C–C bond length is 1.273 Å between the typical double bond (1.35 Å in ethylene) and triple bond (1.21 Å in acetylene). Ionization led to an increase in the C–C bonding and the Si–Si bond length stretched to 2.361 Å (typical single bond value). Following this, is a close lying



Fig. 12.  $\text{Si}_3\text{C}_4$  cationic clusters.Fig. 13.  $\text{Si}_4\text{C}$  cationic clusters.

3D structure (Fig. C.3.4.2) based on the most stable structure found in  $\text{Si}_3\text{C}_3$  cluster, a pyramid-like structure with  $C_s$  symmetry. It is just 0.04 eV above the minimum. The carbon bonds are relaxed in this structure (1.612 Å, 1.612 Å, 1.387 Å, 1.387 Å). The Si–Si distance is 2.962 Å, too large for any kind of bonding. The next stable structure is also 3D (Fig. C.3.4.3) with carbon atoms arranged in planar trapezoidal shape and an energy 0.598 eV above the ground state structure. Other low lying structures observed for this cluster (Fig. 12) are mostly linear or planar. Owing to the large cluster size, many isomers are possible. For the sake of brevity, we have reported here only the low-lying isomers. It is important to note that this cluster has isomers preferring planar geometry. In contrast to other small clusters like  $\text{Si}_2\text{C}_3$  or  $\text{Si}_2\text{C}_4$ , the stability no longer is dependent on formation of multiple C–C bonds. It is dependent on the coordination of the silicon atoms in the cluster. As this is a carbon-rich cluster we see mostly  $sp^2$  hybridization, with some  $sp^3$  hybridization. Our calculated frequencies for the ground state structure are given in Table 17.

### 3.4 $\text{Si}_4\text{C}_n$ cations

#### 3.4.1 $\text{Si}_4\text{C}^+$

We investigated various geometries and report here *six* most stable isomers. The initial geometries for the iso-

mers were based on  $\text{Si}_4^+$ ,  $\text{Si}_5^+$ , and  $\text{C}_5^+$  clusters. The most stable structure based on the  $\text{Si}_5^+$  ground state is found to be a 3D rhombus with a carbon atom at the apex (Fig. C.4.1.1). The Si–Si bond lengths are 2.457 Å and all SiC bonds are 1.86 Å. Mulliken charge distribution shows the four silicon atoms carry symmetrical charges of (0.250e, 0.186e) and the carbon atom, a slight positive charge (0.125e). Pascoli et al. [34] obtained a similar structure as the ground state, but as a quasi-rhombus with a large negative charge of (−0.99e) for the carbon atom. Since we obtained a more symmetrical structure the charges are distributed in a more symmetric fashion. A close lying isomer, a planar structure, is just 0.072 eV above (Fig. C.4.1.2).

However, frequency analysis shows that the second most stable structure has an imaginary frequency and is not a local minimum. Also, another planar structure (Fig. C.4.1.3) is 0.572 eV above than the ground state structure. It is interesting to note that this structure consisting of a  $\text{Si}_2\text{C}$  sub-molecule is more stable than another planar (Fig. C.4.1.4) structure with a  $\text{Si}_3$  sub-molecule. We observed same ordering in the case of neutral clusters. As expected, these silicon rich clusters prefer three-dimensional bonding as compared to linear or planar structures and a major reason contributing to the stability is the formation of several Si–C bonds followed by Si–Si bonds. The frequencies are given in Table 17.

**Table 12.** Electronic states, relative energies, binding energies/atom, and adiabatic ionization potentials (all in eV) for  $\text{Si}_3\text{C}_4^+$  clusters.

Structure	State	$\Delta E$	$E_b$	$AIP$
C.3.4.1	$^2A''$	0.000	5.735	8.809
C.3.4.2	$^2B_2$	0.040	5.730	7.190
C.3.4.3	$^2A_1$	0.598	5.650	7.828
C.3.4.4	$^2B_1$	1.078	5.581	8.069
C.3.4.5	$^2\Sigma_u$	1.475	5.525	7.862
C.3.4.6	$^2B_1$	1.528	5.517	8.532
C.3.4.7	$^2A'$	2.702	5.349	7.918
C.3.4.8	$^2B_1$	3.001	5.307	7.633
C.3.4.9	$^2B_1$	3.593	5.222	8.407

**Table 13.** Electronic states, relative energies, binding energies/atom, and adiabatic ionization potentials (all in eV) for  $\text{Si}_4\text{C}^+$  clusters.

Structure	State	$\Delta E$	$E_b$	$AIP$
C.4.1.1	$^2B_1$	0.000	4.551	10.280
C.4.1.2	$^2A_2$	0.072	4.537	7.550
C.4.1.3	$^2B_1$	0.572	4.437	8.007
C.4.1.4	$^4A_2$	2.899	3.972	8.962
C.4.1.5	$^2B_1$	5.026	3.546	8.776
C.4.1.6	$^4A_2$	5.615	3.314	8.614
C.4.1.7	$^2\Pi$	7.201	3.111	8.683

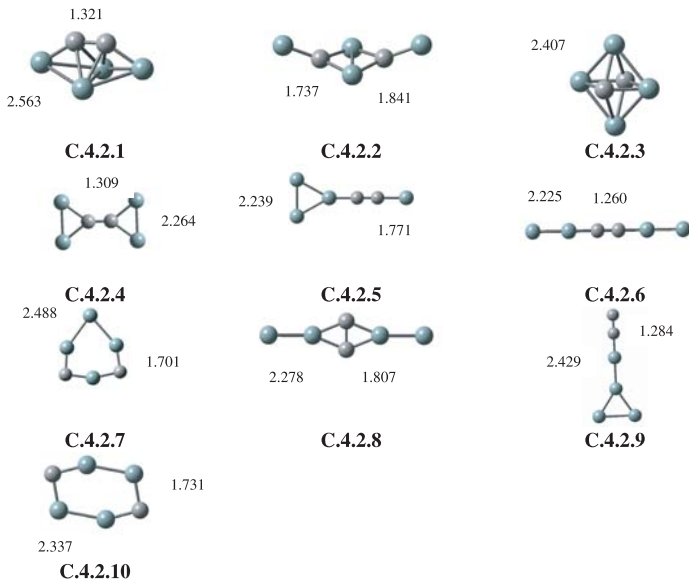


Fig. 14.  $\text{Si}_4\text{C}_2$  cationic clusters.

### 3.4.2 $\text{Si}_4\text{C}_2^+$

We studied various structures including both two-dimensional as well as three-dimensional geometries. The initial geometries for the isomers were based on  $\text{Si}_6^+$  and  $\text{C}_6^+$  clusters. The ground state structure of  $\text{Si}_4\text{C}_2^+$  can be viewed as a  $\text{Si}_4$  tetrahedron, but with  $\text{C}_2$  capping (Fig. C.4.2.1). The C–C bond length is 1.321 Å, between typical double (1.35 Å in ethylene) and triple (1.21 Å in acetylene) bond length value. A similar structure was observed for the neutral species but with a shorter C–C bond length of 1.307 Å [24]. Ionization led to increase in the C–C bond length. Mulliken charge distribution shows that all four Si atoms are all positively charged (0.199e and 0.317e), and the two carbons are slightly negatively charged (−0.016e). Next, 0.678 eV above is another 3D structure (Fig. C.4.2.2) derived from  $\text{Si}_2\text{C}_2$  planar rhombic isomer with Si atoms at the end. The Si–C bonds in the rhombic subsystem are lengthened as compared to the  $\text{Si}_2\text{C}_2$  isomer and appear to be strongly polarized. The silicon atoms have positive charge (0.55e) whereas carbon atoms are quasi-anionic (−0.669e). The frequency analysis shows all real vibrational frequencies for this isomer, indicating it is a local minimum of the energy surface. Next, 1.245 eV above is another 3D structure; a trigonal bipyramid with two carbon atoms capping (Fig. C.4.2.3) with  $\text{C}_{2v}$  symmetry. Similar structure was observed for the neutral clusters [24]. A dumbbell shaped planar structure (Fig. C.4.2.4) observed as the second most stable structure by Pascoli et al. [34] appears to be 1.810 eV above the minimum. The C–C bond length for this planar isomer is smaller than the one obtained in the ground state 3D structure (Fig. C.4.2.1). The other low-lying isomers of  $\text{Si}_4\text{C}_2^+$  located higher in energy are shown in Figure 14. Most of the low-lying isomers have

Table 14. Electronic states, relative energies, binding energies/atom, and adiabatic ionization potentials (all in eV) for  $\text{Si}_4\text{C}_2^+$  clusters.

Structure	State	$\Delta E$	$E_b$	AIP
C.4.2.1	$^2\text{A}_1$	0.000	5.137	8.523
C.4.2.2	$^2\text{A}''$	0.678	5.024	5.383
C.4.2.3	$^2\text{B}_2$	1.245	4.929	9.428
C.4.2.4	$^2\text{B}_{1u}$	1.810	4.835	7.692
C.4.2.5	$^4\text{A}_2$	2.836	4.664	8.518
C.4.2.6	$^2\Pi_g$	3.854	4.495	7.949
C.4.2.7	$^2\text{A}''$	4.578	4.374	8.497
C.4.2.8	$^2\text{B}_{2u}$	4.792	4.338	7.788
C.4.2.9	$^2\text{A}_1$	5.243	4.263	8.674
C.4.2.10	$^4\text{A}_u$	5.674	4.191	10.390

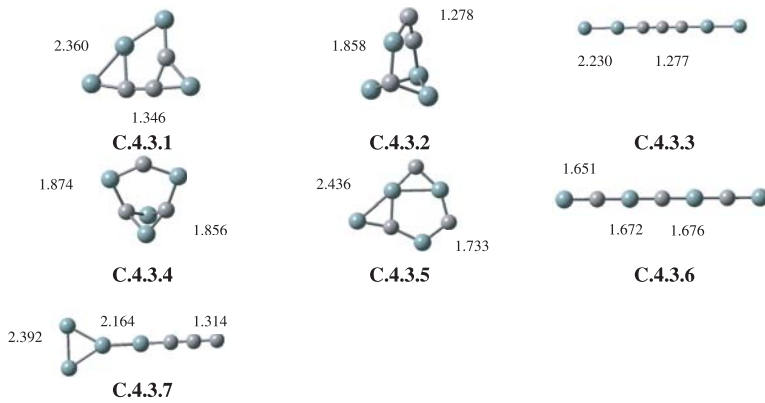
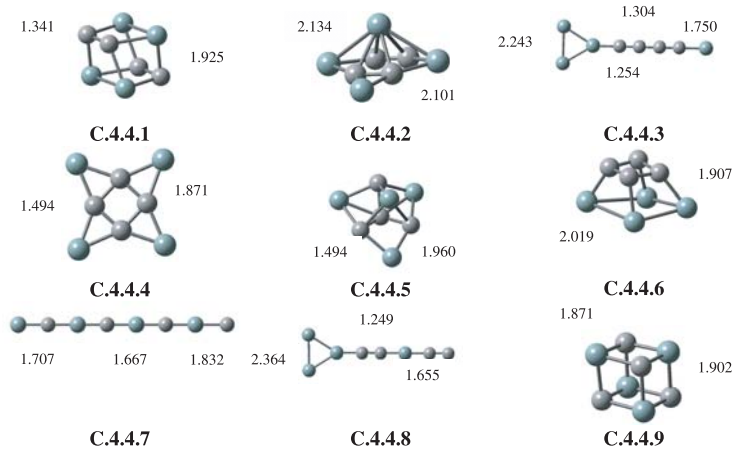
symmetrical distribution of charges and as many as four imaginary frequencies.

### 3.4.3 $\text{Si}_4\text{C}_3^+$

There are *no* studies in the literature about this cluster. We examined various planar, quasi-planar and 3D structures based on the neutral geometry. The ground state structure is a triangular planar pyramid-like structure (Fig. C.4.3.1). A similar structure was found to be the ground state structure in the case of the neutral species [24]. The C–C bond lengths are 1.346 Å (double bond) and 1.499 Å (single bond). The Si–Si linkage is 2.360 Å indicating a single bond formation. The next structure is a 3D structure (Fig. C.4.3.2) at 0.195 eV above the ground minima. The C–C bond length is 1.278 Å. Several Si–C bonds and strong C–C bond of 1.278 Å contribute to the stability of this structure. Among the chain structures silicon terminated chains are found to be more stable than carbon terminated chains. A chain structure with three carbon atoms in center (Fig. C.4.3.3) and C–C bonds each of 1.277 Å in length is 0.565 eV above the minimum and is the most stable among the linear chains. Other less stable planar structures are also shown in Figure 15. In general low-lying  $\text{Si}_4\text{C}_3$  structures tend to be planar. This is also true for the neutral species [24]. Carbon atoms play an important role in stabilizing these structures into planar and quasi-planar geometries. Most of the 3D geometries considered for this particular cluster turned out to be open-ended at the end of optimization process. Our frequencies are given in Table 17.

### 3.4.4 $\text{Si}_4\text{C}_4^+$

There are also *no* studies in the literature about this cluster. We have studied various isomers and report here

Fig. 15.  $\text{Si}_4\text{C}_3$  cationic clusters.Fig. 16.  $\text{Si}_4\text{C}_4$  cationic clusters.

the most stable isomers. As previously observed when the number of silicon atoms is equal to number of carbon atoms, symmetry of a particular cluster played an important role in the overall stability. We obtained a 3D cube-like structure (Fig. C.4.4.1) in  $^2\text{A}$  electronic state is the most stable structure. There is a formation of two C–C bonds, of 1.341 Å each. The SiC linkage is 1.925 Å. The Si–Si distance is 2.50 Å (can form a stretched Si–Si bond). Next, is another 3D pyramid-like structure (Fig. C.4.4.2) with a  $\text{Si}_3$  sub-molecule 0.372 eV above the ground state. This structure was found to be the most stable structure in case of the neutral clusters. Next, about 0.536 eV above is a T-shaped planar structure (Fig. C.4.4.3) with four carbon atoms in a row with C–C bond lengths of 1.254 Å, 1.304 Å, and 1.254 Å, respectively. Silicon termination contributes towards the high stability of this structure. Following in the energetic ordering is a planar star-shaped structure (0.558 eV above) with four C–C bonds of 1.494 Å. With increasing cluster size, the formation of C–C bonds and several strong SiC bonds contribute towards the stability of the cluster. Several other planar and linear structures were observed as shown in Figure 16. Our theoretical frequencies for the most stable structure are given in Table 17.

**Table 15.** Electronic states, relative energies, binding energies/atom, and adiabatic ionization potentials (all in eV) for  $\text{Si}_4\text{C}_3^+$  clusters.

Structure	State	$\Delta E$	$E_b$	AIP
C.4.3.1	$^2\text{A}''$	0.000	5.418	8.216
C.4.3.2	$^2\text{A}$	0.195	5.390	6.391
C.4.3.3	$^2\text{A}$	0.565	5.337	7.082
C.4.3.4	$^4\text{A}$	2.769	5.022	8.636
C.4.3.5	$^2\Pi_u$	3.105	4.974	7.866
C.4.3.6	$^4\text{A}''$	3.383	4.935	9.244
C.4.3.7	$^2\text{A}$	3.603	4.903	7.863
C.4.3.8	$^2\Pi_u$	3.973	4.851	8.612
C.4.3.9	$^4\text{A}_2$	5.510	4.631	8.722

**Table 16.** Electronic states, relative energies, binding energies/atom, and adiabatic ionization potentials (all in eV) for  $\text{Si}_4\text{C}_4^+$  clusters.

Structure	State	$\Delta E$	$E_b$	AIP
C.4.4.1	$^2\text{A}$	0.000	5.543	7.658
C.4.4.2	$^2\text{A}'$	0.372	5.497	9.649
C.4.4.3	$^4\text{A}_2$	0.536	5.476	8.314
C.4.4.4	$^2\text{B}_{1u}$	0.558	5.473	6.172
C.4.4.5	$^4\text{A}$	1.931	5.302	8.041
C.4.4.6	$^4\text{A}$	2.058	5.286	8.538
C.4.4.7	$^2\Pi_u$	2.692	5.206	7.373
C.4.4.8	$^2\text{A}_1$	3.791	5.069	8.236
C.4.4.9	$^4\text{A}$	4.160	5.023	9.061

## 4 Discussions

### 4.1 Bonding and energetics

We now summarize the major trends observed for the lowest energy isomers. For the  $\text{SiC}_n^+$  series all structures are cyclic, whereas for the  $\text{Si}_2\text{C}_n^+$  series we have linear chains as the ground state structures. For the chain structures silicon always preferred terminal position, indicating preference for  $sp$  hybridization. For the  $\text{Si}_3\text{C}_n^+$  series all structures are planar while in the  $\text{Si}_4\text{C}_n^+$  series  $\text{Si}_4\text{C}^+$ ,  $\text{Si}_4\text{C}_2^+$  and  $\text{Si}_4\text{C}_4^+$  are 3D while  $\text{Si}_4\text{C}_3^+$  is quasi-planar. In the neutral species [24] the most stable structure  $\text{Si}_3\text{C}_3$  was a 3D structure with multi-centered bonding. This structure had high cohesion and co-ordination. After ionization the  $\text{Si}_3\text{C}_3^+$  cluster was found to be planar. The dimensionality of this cluster reduced from 3D to 2D. Ionization leads to increases in SiC bond lengths and decreases in C–C bond lengths, although the decrement in C–C bonds is much higher than the increment in SiC bonds.

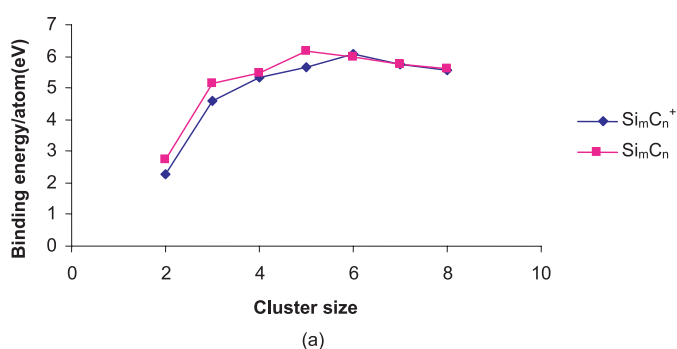
Figure 17a shows the size dependence of the binding energy per atom for the most stable isomers of  $\text{Si}_m\text{C}_n^+$  cationic clusters. For comparison, the size dependence of the corresponding stable neutral isomers is also shown.

**Table 17.** Harmonic vibrational frequencies (in  $\text{cm}^{-1}$ ) for the ground state  $\text{Si}_m\text{C}_n$  cationic clusters. Results are compared with the theoretical frequencies for identical structures.

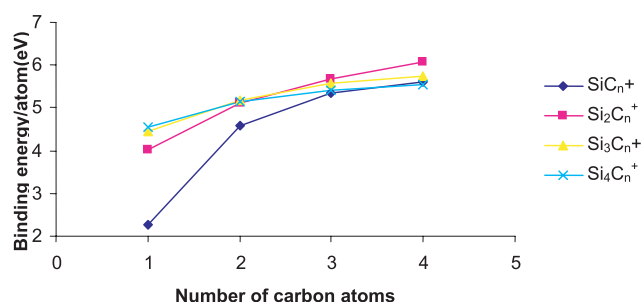
Cluster	Vibrational frequencies	
$\text{SiC}^+$ $C_v$	808.0	890 [38]
$\text{SiC}_2^+$ $C_{2v}$	253.7, 610.9, 1830.9	250, 607, 1831 [34]
$\text{SiC}_3^+$ $C_{2v}$	269.5, 440.9, 573.9, 889.4, 1290.9, 1615.2	294, 434, 583, 883, 1310, 1636 [34]
$\text{SiC}_4^+$ $C_{2v}$	210.2, 276.8, 418.9, 493.6, 505.4, 539.2, 1098.5, 1755.5, 1906.0	484i, 209i, 344, 349, 441, 467, 1122, 1683, 1941 [34]
$\text{Si}_2\text{C}^+$ $D_{\infty h}$	102.8, 102.8, 572.3, 1289.9	81, 705, 1931 [34]
$\text{Si}_2\text{C}_2^+$ $D_{2h}$	85.5, 108.6, 233.6, 448.5, 803.2, 1959.5	96, 115, 199, 297, 453, 789, 1989 [34] 105, 122, 218, 303, 447, 776, 1953 [16]
$\text{Si}_2\text{C}_3^+$ $D_{\infty h}$	67.5, 67.9, 162.9, 178.5, 424.3, 437.0, 447.2, 801.7, 1525.4, 1969.7	79, 187, 443, 498, 812, 1535, 1878 [28]
$\text{Si}_2\text{C}_4^+$ $D_{\infty h}$	59.3, 66.0, 137.7, 161.4, 320.9, 350.4, 396.5, 550.2, 678.5, 717.0, 1212.4, 1945.8, 2117.5	61, 67, 142, 167, 318, 349, 396, 505, 662, 667, 1204, 1969, 2103 [34]
$\text{Si}_3\text{C}^+$ $C_{2v}$	63.5, 140.4, 182.3, 501.5, 723.5, 1017.9	49, 169, 187, 509, 696, 1016 [34]
$\text{Si}_3\text{C}_2^+$ $C_{2v}$	113.5, 151.7, 195.7, 321.2, 432.7, 568.9, 637.6, 876.4, 1642.1	103, 122, 124, 348, 441, 538, 591, 911, 1632 [34]
$\text{Si}_3\text{C}_3^+$ $C_{2v}$	57.9, 71.4, 143.2, 194.5, 247.6, 371.0, 434.9, 483.5, 573.2, 785.7, 1417.0, 2057.2	
$\text{Si}_3\text{C}_4^+$ $C_s$	58.7, 105.1, 173.9, 238.8, 303.4, 310.3, 330.4, 398.3, 434.5, 491.4, 529.8, 756.0, 816.6, 1739.6, 1796.7	
$\text{Si}_4\text{C}^+$ $C_{2v}$	147.2, 163.1, 208.4, 222.9, 251.7, 360.4, 599.5, 807.2, 875.6, 599.5, 807.2, 875.6	
$\text{Si}_4\text{C}_2^+$ $C_{2v}$	146.4, 159.6, 214.5, 386.4, 426.6, 526.3, 616.4, 822.8, 1593.1	123, 126, 151, 231, 238, 332, 380, 421, 528, 581, 881, 1589 [34]
$\text{Si}_4\text{C}_3^+$ $C_s$	83.7, 136.0, 165.4, 210.4, 235.8, 247.7, 353.5, 431.8, 441.1, 492.6, 603.4, 656.9, 860.8, 1033.6, 1509.8	
$\text{Si}_4\text{C}_4^+$ $C_1$	119.7, 194.7, 263.7, 298.5, 310.2, 348.7, 355.0, 374.8, 390.9, 414.9, 421.3, 563.9, 598.6, 605.2, 628.2, 639.4, 1393.9, 1401.8	

In cases where the number of atoms is equal in two clusters, we have chosen the cluster with the higher binding energy per atom. In case of the neutral clusters we see enhanced stabilities at  $n = 3$  and  $n = 5$  whereas for the cationic cluster we see significantly enhanced stability at  $n = 6$ . Figure 17b shows the binding energy per atom vs. the carbon content. As observed in case of neutral clusters [24] for a particular set of clusters with fixed number of silicon atoms, the binding energy per atom usually increases with the increase in the number of carbon atoms. The clusters with equal number of silicon and carbon atoms are usually highly stable. We do observe a noticeable peak for the six-atom cluster  $\text{Si}_2\text{C}_4^+$ . As noted before, this carbon-rich hexa-atomic cluster  $\text{Si}_2\text{C}_4^+$  is a linear chain with three C–C bonds for the ground state structure and the highest binding energy per atom of 6.089 eV. Next, most stable structure is the seven-atom cluster  $\text{Si}_3\text{C}_4^+$ . The ground state structure is a planar structure with two C–C bonds and a binding energy per atom of 5.735 eV. In general, all these clusters exhibit high binding energies similar to their neutral counterparts.

We also calculated the fragmentation energies of the ground state cationic clusters into different possible binary channels. These are not reported here, in tabular form, for the sake of brevity. Out of sixteen clusters, eleven of them decays into channels in which one fragment is a  $\text{Si}^+$  atom, four into channels in which one fragment is a Si atom. Thus, in general, the preferred mode of decay for SiC cations carries either a positively charged silicon atom or a neutral silicon atom. This is to be expected, given the fact that the ionization potential for Si is 3.1 eV lower than C. Mass spectroscopic experiments by Parent [37] also showed  $\text{Si}^+$  as the abundant species. Figure 18b shows the graph of bond dissociation energy versus the number of carbon atoms. The  $\text{SiC}_n^+$  and  $\text{Si}_2\text{C}_n^+$  series show an even-odd oscillatory behavior with peaks at odd and even number of clusters respectively. In Figure 18a as well as 18b we can see that for  $\text{Si}_3\text{C}_n^+$  and  $\text{Si}_4\text{C}_n^+$  species, the stability tends to decrease with increase in cluster size / carbon content. The  $\text{Si}_2\text{C}^+$  cluster has the highest dissociation energy of 6.581 eV. The cationic species have lesser dissociation energies than the neutral species.

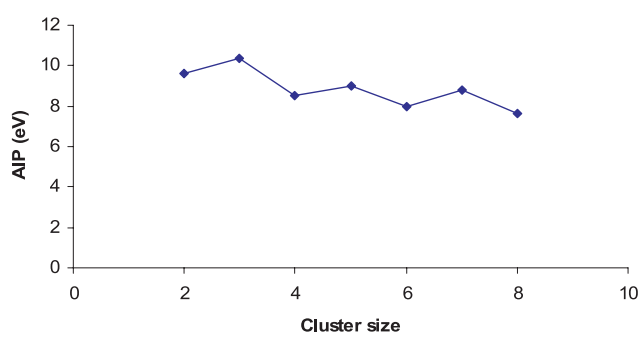


(a)

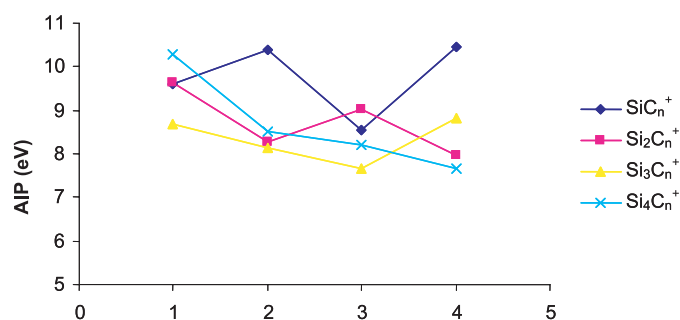


(b)

**Fig. 17.** Binding energy per atom (in eV) versus (a) the cluster size and (b) the number of carbon atoms in the cluster.

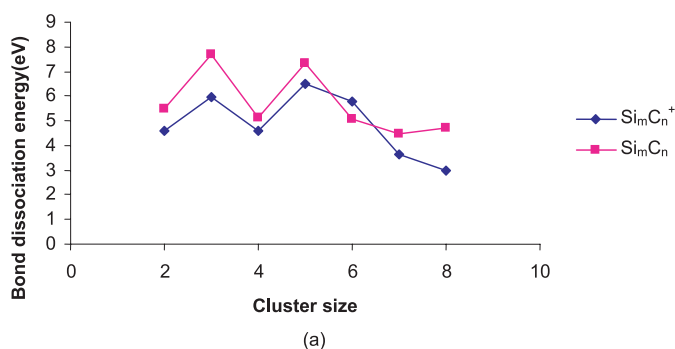


(a)

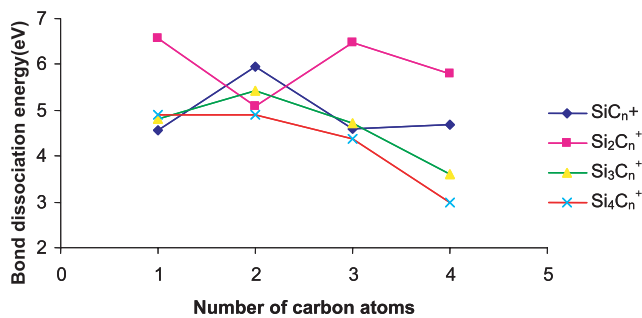


(b)

**Fig. 19.** Adiabatic ionization potential (in eV) versus (a) the cluster size and (b) the number of carbon atoms in the cluster.



(a)



(b)

**Fig. 18.** Bond dissociation energy (in eV) versus (a) the cluster size and (b) the number of carbon atoms in the cluster.

## 4.2 Adiabatic ionization potentials

The adiabatic ionization potentials (*AIP*) of the clusters are also shown in Tables 1–16 and the results have been compared with available results in the literature wherever possible. Parent [37] by bracketing technique estimated the ionization potentials of two forms of  $\text{Si}_2\text{C}_2^+$  in the study of charge transfer reactions between the ion and the neutral. Their adiabatic ionization potentials for the rhombic (Fig. C.2.2.3) and linear (Fig. C.2.2.1) forms are given in Table 6. Our values indicate slight overestimations of the *AIP*'s from experimental [37] and theoretical [38] results, but follow the same trends. Jiang et al. [35] report that for the  $\text{SiC}_n^+$  and  $\text{Si}_2\text{C}_n^+$  ( $n = 1-7$ ) series the IP values peak for cluster size = 3. On  $\text{SiC}_{m-1}^+$  ( $m = 3-16$ ) series Wu et al. [35] have claimed that for odd  $m$  the IP's values peak for  $m < 13$ . Both studies conclude that the stability decreases with increase in cluster size. We have shown our adiabatic ionization potentials as a function of cluster size in Figure 19. The saw-tooth behavior is indicated by higher IP's for odd number of atoms:  $\text{SiC}_2^+$ ,  $\text{Si}_2\text{C}_3^+$  and  $\text{Si}_3\text{C}_4^+$ . The five-atom cluster  $\text{SiC}_4^+$  has highest ionization potential of 10.445 eV. As indicated in Figure 19b, the  $\text{SiC}_n^+$  and  $\text{Si}_2\text{C}_n^+$  series show an even-odd oscillatory behavior with peaks at odd and even number of clusters respectively.

## 5 Conclusions

In this work, we have reported a comprehensive study of the geometric, energetic, and bonding properties of cationic hetero-atomic silicon-carbide clusters using the theoretical formalism of LDA-DFT. Energetic properties show that the stability, from the point of view of binding energy per atom, shows an oscillatory pattern with cluster size. However, carbon-rich species tend to be more stable. In comparison to the neutral clusters, the cationic species are more open ended structures. In particular, as observed in case of  $\text{Si}_3\text{C}_3^+$  cluster; which was identified as a most stable cluster in the neutral form, ionization led to the reduction in dimensionality. In contrast to the neutral clusters, formation of C–C bonds is not the most important criteria affecting the stability, but stability also largely depends on the charge distribution. For example, in the  $\text{Si}_2\text{C}_n^+$  series, the ground states all have linear geometries and show strong charge oscillation as compared to cyclic structures. Silicon's ability to act as an electron donor play a dominant role in stability.

Finally, the authors gratefully acknowledge partial support from the Welch Foundation, Houston, Texas (Grant No. Y-1525).

## References

1. *Atomic and Molecular Clusters*, edited by E.R. Bernstein (Elsevier, New York, 1990)
2. *Physics and Chemistry of Finite Systems – From Clusters to Crystals: Proceedings of the NATO Advanced Research Workshop*, edited by P. Jena, S.N. Khanna, B.K. Rao (Kluwer Academic Publishing, 1991)
3. *Clusters of Atoms and Molecules*, edited by H. Haberland (Springer-Verlag, Berlin, 1994)
4. U. Naher, S. Bjornholm, S. Frauendorf, F. Garcias, C. Guet, *Phys. Rep.* **285**, 245 (1997)
5. S. Sugano, H. Koizumi, *Microcluster Physics* (Springer-Verlag, New York, 1998)
6. *Theory of Atomic and Molecular Clusters: With a Glimpse at Experiments*, edited by J. Jellinek, R.S. Berry, J. Jortner (Springer-Verlag, New York, 1999)
7. S. Bjornholm, J. Borggreen, *Phil. Mag. B* **79**, 1321 (1999)
8. P. Jena, S.N. Khanna, B.K. Rao, *Theory of Atomic and Molecular Clusters* (Springer-Verlag, Berlin, 1999)
9. R.L. Johnston, R.L. Johnston, *Atomic and Molecular Clusters* (Routledge Publishing, New York, 2002)
10. *Nanostructured Materials and Nanotechnology: Concise Edition*, edited by H.S. Nalwa (Elsevier Science and Technology, New York, 2001); *Silicon-Based Material and Devices: Materials and Processing, Properties and Devices* (Elsevier Science and Technology, New York, 2001)
11. *Nanostructured Silicon-Based Powders and Composites*, edited by A.P. Legrand, C. Senemaud, A. Legrand, C. Senemaud (Routledge Publishing, New York, 2002)
12. *Microcrystalline and Nanocrystalline Semiconductors – 2000: Materials Research Society Symposium Proceedings*, edited by P.M. Fauchet, N. Koshida, J.M. Buriak, L.T. Canham, B.E. White (Materials Research Society, 2001)
13. *Nanostructured Materials*, edited by J.Y.-R. Ying (Academic Press, 2001)
14. M.N. Huda, A.K. Ray, *Phys. Rev. A* **69**, 011201 (2004); *Virtual Journal of Nanoscale Science and Technology*, Feb. 9 (2004); M.N. Huda, A.K. Ray, *Eur. Phys. J. D* **31**, 63 (2004)
15. M. Bertolus, V. Brenner, P. Millie, *Eur. Phys. J. D* **1**, 197 (1998); M. Bertolus, F. Finocchi, P. Mille, *J. Chem. Phys.* **120**, 4333 (2004)
16. R.S. Grev, H.F. Schaefer III, *J. Chem. Phys.* **80**, 3553 (1984); I.M.B. Nielsen, W.D. Allen, A.G. Csaszar, H.F. Schaefer III, *J. Chem. Phys.* **107**, 1195 (1997); J.P. Kenny, W.D. Allen, H.F. Schaefer III, *J. Chem. Phys.* **118**, 7353 (2003); I.L. Alberts, R.S. Grev, H.F. Schaefer III, *J. Chem. Phys.* **93**, 5046 (1990); R. Grev, H. Schaefer III, *J. Chem. Phys.* **82**, 4126 (1985); E. Bolton, B. DeLeeuw, J. Fowler, R. Grev, H. Schaefer III, *J. Chem. Phys.* **97**, 5586 (1992); I. Ignatyev, H.F. Schaefer III, *J. Chem. Phys.* **103**, 7025 (1995)
17. J. Oddershede, J.R. Sabin, G.H.F. Diercksen, N.E. Gruner, *J. Chem. Phys.* **83**, 1702 (1985); A.J. Sadlej, G.H.F. Diercksen, J. Oddershede, J.R. Sabin, *Chem. Phys.* **122**, 297 (1988); G.H.F. Diercksen, N.F. Gruner, J. Oddershede, J.R. Sabin, *Chem. Phys. Lett.* **117**, 29 (1985)
18. M.C. McCarthy, A.J. Apponi, P. Thaddeus, *J. Chem. Phys.* **111**, 7175 (1999); V.D. Gordon, E.S. Nathan, A.J. Apponi, M.C. McCarthy, P. Thaddeus, *J. Chem. Phys.* **113**, 5311 (2000)
19. C.M.L. Rittby, *J. Chem. Phys.* **95**, 5609 (1991); C.M.L. Rittby, *J. Chem. Phys.* **100**, 175 (1994); C.M.L. Rittby, *J. Chem. Phys.* **96**, 6768 (1992)
20. G.W. Trucks, R.J. Bartlett, *J. Mol. Struct. (Theochem)* **135**, 423 (1986); G.B. Fitzgerald, R.J. Bartlett, *Int. J. Quant. Chem.* **38**, 121 (1990); G.B. Fitzgerald, S.J. Cole, R.J. Bartlett, *J. Chem. Phys.* **85**, 1701 (1986)
21. J.D. Presilla-Márquez, S.C. Gay, C.M.L. Rittby, W.R.M. Graham, *J. Chem. Phys.* **102**, 6354 (1995); J.D. Presilla-Márquez, C.M.L. Rittby, W.R.M. Graham, *J. Chem. Phys.* **104**, 2818 (1996); J.D. Presilla-Márquez, W.R.M. Graham, *J. Chem. Phys.* **100**, 181 (1993)
22. X. Duan, L.W. Burggraf, D. Weeks, *J. Chem. Phys.* **116**, 3601 (2002)
23. G.E. Froudakis, A.D. Zdetsis, M. Muhlhauser, B. Engels, S.D. Peyerimhoff, *J. Chem. Phys.* **101**, 6790 (1994); G.E. Froudakis, M. Muhlhauser, A.D. Zdetsis, *Chem. Phys. Lett.* **233**, 619 (1995); M. Muhlhauser, G.E. Froudakis, A.D. Zdetsis, S.D. Peyerimhoff, *Chem. Phys. Lett.* **204**, 617 (1993); M. Muhlhauser, G.E. Froudakis, A.D. Zdetsis, B. Engels, N. Flytzanis, S.D. Peyerimhoff, *Z. Phys. D* **32**, 113 (1994); A.D. Zdetsis, G.E. Froudakis, M. Muhlhauser, H. Thummler, *J. Chem. Phys.* **104**, 2566 (1996)
24. P. Pradhan, A.K. Ray, *J. Mol. Struct. (Theochem)* **716**, 109 (2004)
25. R.G. Parr, W. Yang, *Density Functional Theory of Atoms and Molecules* (Oxford University Press, New York, 1989)
26. P. Hohenberg, W. Kohn, *Phys. Rev.* **136**, B864 (1964); W. Kohn, L.J. Sham, *Phys. Rev.* **140**, A1133 (1965); D.M. Ceperley, B.J. Adler, *Phys. Rev. Lett.* **45**, 566 (1980)
27. R.O. Jones, O. Gunnarsson, *Rev. Mod. Phys.* **61**, 689 (1989)
28. J.C. Slater, *Quantum Theory of Molecules and Solids*, Vol. 4: The Self-Consistent-Field for Molecules and Solids

- (McGraw-Hill, New York, 1974); S.H. Vosko, L. Wilk, M. Nusair, *Can. J. Phys.* **58**, 1200 (1980)
29. W.J. Hehre, L. Radom, P.V.R. Schleyer, J.A. Pople, *Ab Initio Molecular Orbital Theory* (Wiley, New York, 1986)
30. Gaussian '03 (Revision A.1), M.J. Frisch et al., Gaussian Inc., Pittsburgh PA (2003)
31. J.B. Foresman, A.E. Frisch, *Exploring Chemistry with Electronic Structure Methods*, 2nd edn. (Gaussian, Inc. Pittsburgh, PA, 1996)
32. R.S. Mulliken, *J. Chem. Phys.* **23**, 1833 (1955); R.S. Mulliken, *J. Chem. Phys.* **23**, 1841 (1955); R.S. Mulliken, *J. Chem. Phys.* **23**, 2343 (1955)
33. J.R. Flores, A. Largo-Cabrerizo, J. Largo-Cabrerizo, *Chem. Phys. Lett.* **140**, 26 (1987); J.R. Flores, A. Largo, *Chem. Phys.* **140**, 19 (1990)
34. H. Lavendy, J.M. Robbe, J.P. Flament, G. Pascoli, *J. Chim. Phys.* **94**, 649 (1997); H. Lavendy, J.M. Robbe, J.P. Flament, G. Pascoli, *J. Chim. Phys.* **94**, 1779 (1997); G. Pascoli, H. Lavendy, *Int. J. Mass Spec.* **173**, 41 (1998); H. Lavendy, J.M. Robbe, J.P. Flament, G. Pascoli, *J. Chim. Phys.* **177**, 31 (1998)
35. H. Wu, Z. Jiang, X. Xu, F. Zhang, Z. Jin, *J. Mol. Struct. (Theochem)* **620**, 9 (2003); Z. Jiang, X. Xu, H. Wu, F. Zhang, Z. Jin, *J. Mol. Struct. (Theochem)* **624**, 61 (2003)
36. D.L. Michalopoulos, M.E. Geusic, P.R.R. Langridge-Smith, R.E. Smalley, *J. Chem. Phys.* **80**, 3556 (1984)
37. D.C. Parent, *Int. J. Mass Spec. Ion Proc.* **116**, 257 (1992); D.C. Parent, *Int. J. Mass Spec. Ion Proc.* **138**, 307 (1994)
38. A.I. Boldyrev, J. Simons, V.G. Zakrzewski, W. von Niessen, *J. Phys. Chem.* **98**, 1427 (1994)